Free-Energy Perturbation, Thermodynamic Integration, Potential of Mean Force

(+working examples on chemical reactivity)

Lubomír Rulíšek, Martin Srnec

Institute of Organic Chemistry and Biochemistry AS CR

J. Heyrovský Institute of Physical Chemistry AS CR, Prague, Czech Republic

ÚOCHB AV ČR

J. Heyrovský Institute of Physical Chemistry
Academy of Sciences of the Czech Republic

Outline

Working Examples on Chemical Reactivity

- Computational Investigations of Asymmetric Organocatalysis
- Divergent Pathways and Competitive Mechanisms of Metathesis Reactions between 3-Arylprop-2-ynyl esters and Aldehydes

Simulations of Thermodynamic Properties

- Free-Energy Perturbation
- Thermodynamic Integration
- Potential of Mean Force

En Route to Quantitative Accuracy (~2 kcal.mol^{-1}) in "Computational Catalysis"

Challenges in Computational Homogeneous Catalysis

Accuracy of TS barriers (electronic structure)

Solvation Effects

Conformational Complexity

Nuclear Quantum Effects

Asymmetric Allylation of Aldehydes with Allyltrichlorosilanes

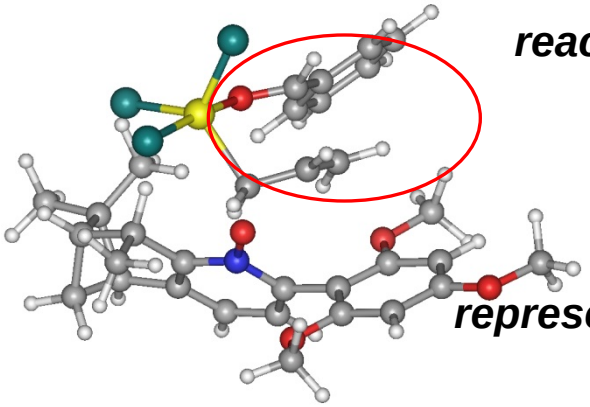

reaction region

representative catalyst (Lewis base)

- **chiral phosphoramides (Denmark, 1994)**
- **axially chiral biquinoline *N,N'*-dioxide (Nakajima)**
- **bipyridine *N,N'*-dioxides and *N,N'N''*-trioxides (Hayashi, Kotora, Kwong, …)**
- **pyridine-derived *N*-monooxides (Kočovský, Malkov)**
- **"non-pyridine-type" *N*-monooxide derived from proline (Hoveyda)**
- ***N*-oxides derived from tetrahydroisoquinolines (Govender)**
- **sulfoxides, sulfonamides, phosphine oxides (BINAPO), dinitrones,…**

Computational ingredients:

Conformational Complexity, Dispersion/Solvation Effects, Entropic Effects

Scheme 2. Mechanistic Dichotomy in the Coupling of Allyltrichlorosilane with Benzaldehyde Catalyzed By (*S*)-**1b**[20]

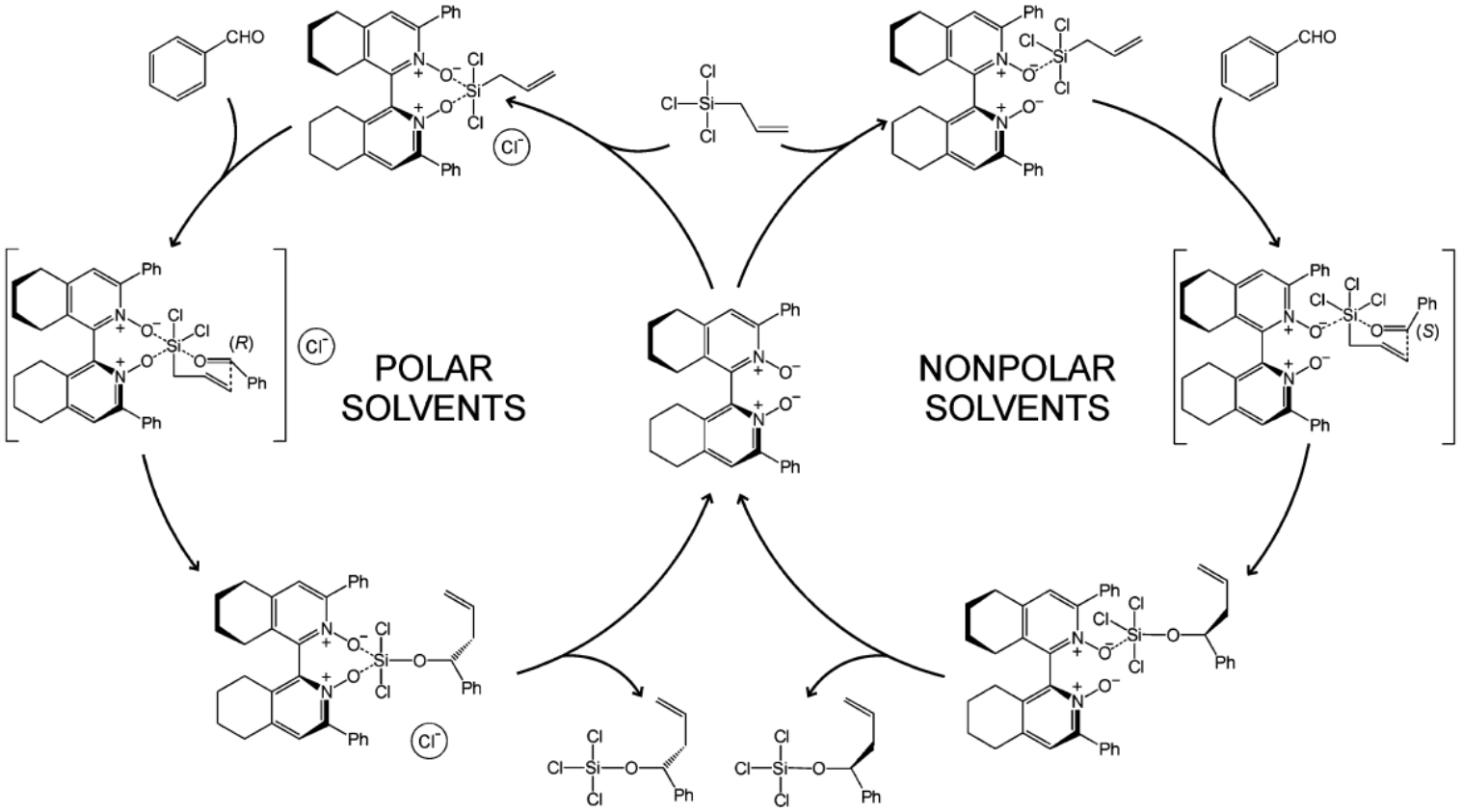

Ducháčková, L; Kadlčíková, A.; Kotora, M. ; Roithová, J.: Oxygen Superbases as Polar Binding Pockets in Nonpolar Solvents. *J. Am. Chem. Soc.* **2010**, *132*, 12660.

Kadlčíková, A.; Valterová, I.; Ducháčková, L; Roithová, J.; Kotora, M.: Lewis Base Catalyzed Enantioselective Allylation of alpha,beta-Unsaturated Aldehydes. *Chem. Eur. J.* **2010**, *16*, 9442.

Hrdina, R.; Opekar, F.; Roithová, J.; Kotora, M.: *Chem. Commun.* **2009**, 2314.

Dissociative (Cationic)/Associative (Mechanism) Solvent-Dependent Enantionselectivity

Table 1 Conductivity measurements

Entry	Solvent[a]	Composition	Conductivity/mV
1	MeCN	**1**	1560
2	MeCN	$AllylSiCl_3$	1510
3	MeCN	**1** + $AllylSiCl_3$	1780
4	MeCN[b]	$AllylSiCl_3$	1560
5	MeCN[b]	**1** + $AllylSiCl_3$	2100
6	CH_2Cl_2	$AllylSiCl_3$	188
7	CH_2Cl_2	**1** + $AllylSiCl_3$	458
8	PhCl	$AllylSiCl_3$	55
9	PhCl	**1** + $AllylSiCl_3$	57
10	EtOAc	$AllylSiCl_3$	62
11	EtOAc	**1** + $AllylSiCl_3$	63

[a] 0.0112 mmol ml^{-1} unless otherwise noted. [b] 0.0224 mmol ml^{-1}.

Hrdina, R.; Opekar, F.; Roithová, J.; Kotora, M.: *Chem. Commun.* **2009**, 2314.

(Possibly) New Mechanism (Polar-pocket or "Enzymatic-like")

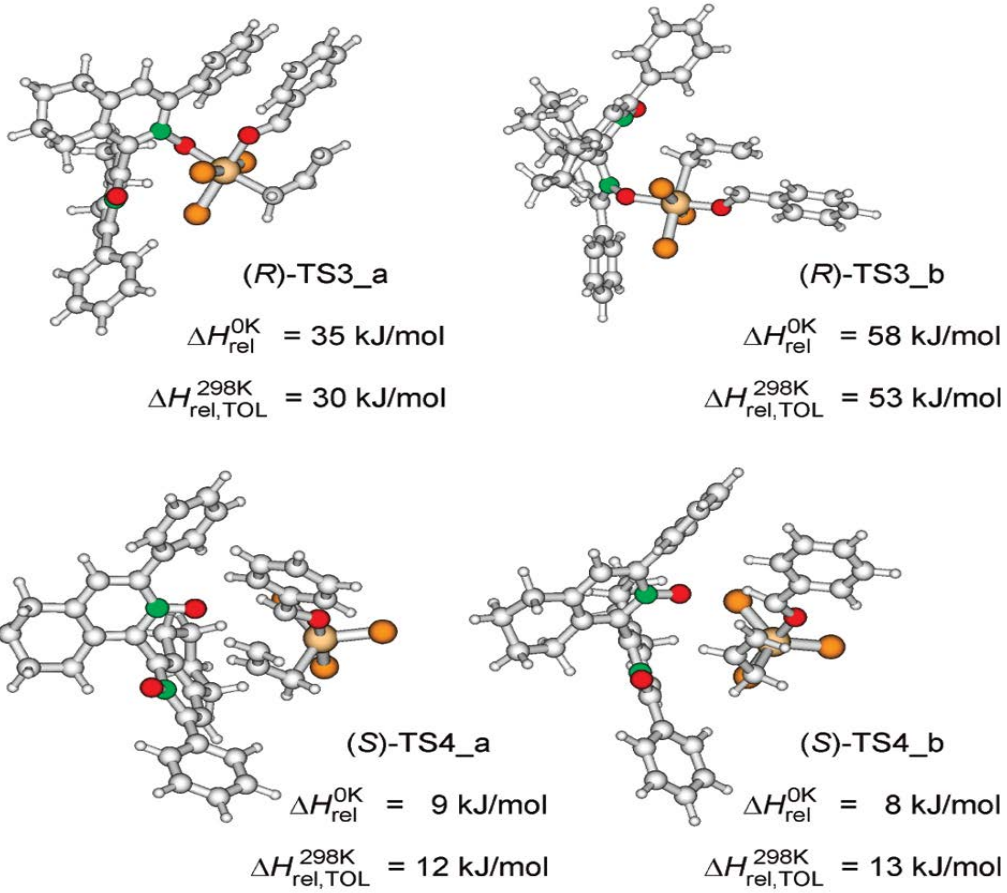

Ducháčková, L; Kadlčíková, A.; Kotora, M. ; Roithová, J.: Oxygen Superbases as Polar Binding Pockets in Nonpolar Solvents. *J. Am. Chem. Soc.* **2010**, *132*, 12660.

Asymmetric Allylation of Aldehydes with Allyltrichlorosilanes

Scheme 1. Allylation of aldehydes **1** with allyl and crotyl trichlorosilanes **2**-**4**.[a]

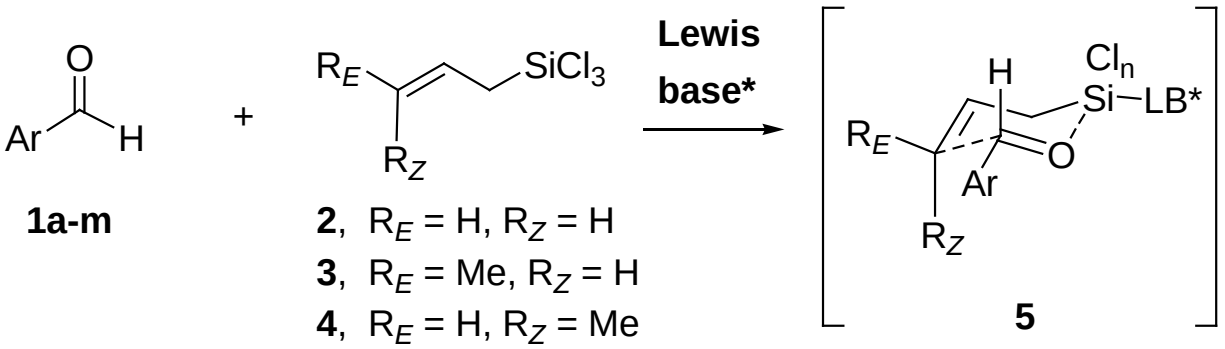

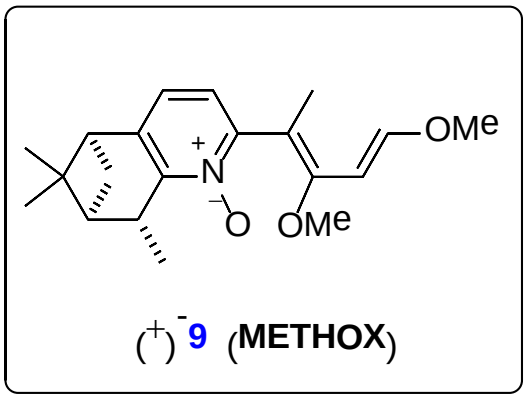

(+)-**9** (**METHOX**)

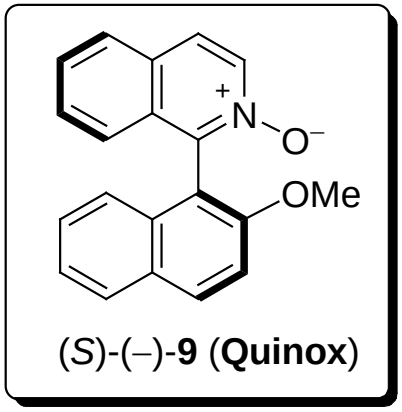

(*S*)-(–)-**9** (**Quinox**)

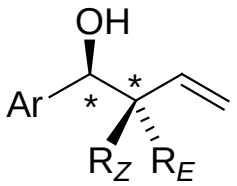

6, R_E = H, R_Z = H
7, R_E = Me, R_Z = H
8, R_E = H, R_Z = Me

[a]For **a**-**m**, see Table 1.

Table: The Allylation of Aldehydes 1a-k with Allyltrichlorosilane 5a Catalyzed by Lewis Bases

Entry	Aldehyde	Ar	Catalyst (mol%)	Solvent	Temp (°C)	Time (h)	Yield (%)[b]	ee (%)[c,d]
1	**1a**	Ph	(+)-**9** (5)	MeCN	-40	18	?95	96 (*S*)
2	**1b**	4-CF_3-C_6H_4	(+)-**9** (5)	MeCN	-40	18	86	93 (*S*)
3	**1c**	4-MeO-C_6H_4	(+)-**9** (5)	MeCN	-40	18	?95	96 (*S*)
4	**1d**	3-MeO-C_6H_4	(+)-**9** (5)	MeCN	-40	18	87	95 (*S*)
5	**1e**	2-MeO-C_6H_4	(+)-**9** (5)	MeCN	-40	18	?95	89 (*S*)
6	**1f**	4-Cl-C_6H_4	(+)-**9** (5)	MeCN	-40	18	80	94 (*S*)
7	**1g**	3-Cl-C_6H_4	(+)-**9** (5)	MeCN	-40	18	81	97 (*S*)
8	**1h**	2-Cl-C_6H_4	(+)-**9** (5)	MeCN	-40	18	75	92 (*S*)
9	**1i**	3,5-Me_2-C_6H_4	(+)-**9** (5)	MeCN	-40	18	0	–
10	**1j**	2,6-Me_2-C_6H_4	(+)-**9** (5)	MeCN	-40	18	0	–
11	**1a**	Ph	(–)-**15e** (10)	$CHCl_3$	-40	18	60	90 (*S*)
12	**1b**	4-CF_3-C_6H_4	(–)-**15e** (10)	$CHCl_3$	-40	18	34	85 (*S*)
13	**1c**	4-MeO-C_6H_4	(–)-**15e** (10)	$CHCl_3$	-40	18	25	91 (*S*)
14	**1e**	2-MeO-C_6H_4	(–)-**15e** (10)	$CHCl_3$	-40	18	53	75 (*S*)
15	**1f**	4-Cl-C_6H_4	(–)-**15e** (10)	$CHCl_3$	-40	18	63	88 (*S*)
16	**1g**	3-Cl-C_6H_4	(–)-**15e** (10)	$CHCl_3$	-40	18	54	89 (*S*)
17	**1h**	2-Cl-C_6H_4	(–)-**15e** (10)	$CHCl_3$	-40	18	75	86 (*S*)
18	**1i**	3,5-Me_2-C_6H_4	(–)-**15e** (10)	MeCN	-20	18	0	?
19	**1a**	Ph	(+)-**16** (5)	MeCN	-20	18	87	72 (*S*)[e]
20	**1k**	4-F-C_6H_4	(+)-**16** (5)	MeCN	-20	18	58	70 (*S*)[e]
21	**1c**	4-MeO-C_6H_4	(+)-**16** (5)	MeCN	-20	18	72	70 (*S*)[e]
22	**1i**	3,5-Me_2-C_6H_4	(+)-**16** (5)	MeCN	-20	18	73	62 (*S*)[e]
23	**1a**	Ph	(+)-**10** (5)	CH_2Cl_2	-40	2	68	87 (*R*)[f]
24	**1b**	4-CF_3-C_6H_4	(+)-**10** (5)	CH_2Cl_2	-40	2	85	96 (*R*)[f]
25	**1c**	4-MeO-C_6H_4	(–)-**10** (5)	CH_2Cl_2	-40	18	70	16 (*S*)[f,g]
26	**1e**	4-MeO-C_6H_4	(+)-**10** (5)	CH_2Cl_2	-20	18	75	72 (*R*)
27	**1e**	4-MeO-C_6H_4	(+)-**10** (5)	CH_2Cl_2	0	18	82	45 (*R*)
26	**1d**	3-MeO-C_6H_4	(+)-**10** (5)	CH_2Cl_2	-40	12	73	80 (*R*)[f]
27	**1e**	2-MeO-C_6H_4	(+)-**10** (5)	CH_2Cl_2	-40	12	40	37 (*R*)[f]
28	**1i**	3,5-Me_2-C_6H_4	(+)-**10** (5)	CH_2Cl_2	-40	16	68	81 (*R*)[h]
29	**1j**	2,6-Me_2-C_6H_4	(+)-**10** (5)	CH_2Cl_2	-40	18	0	–

“Non-catalysed” reaction

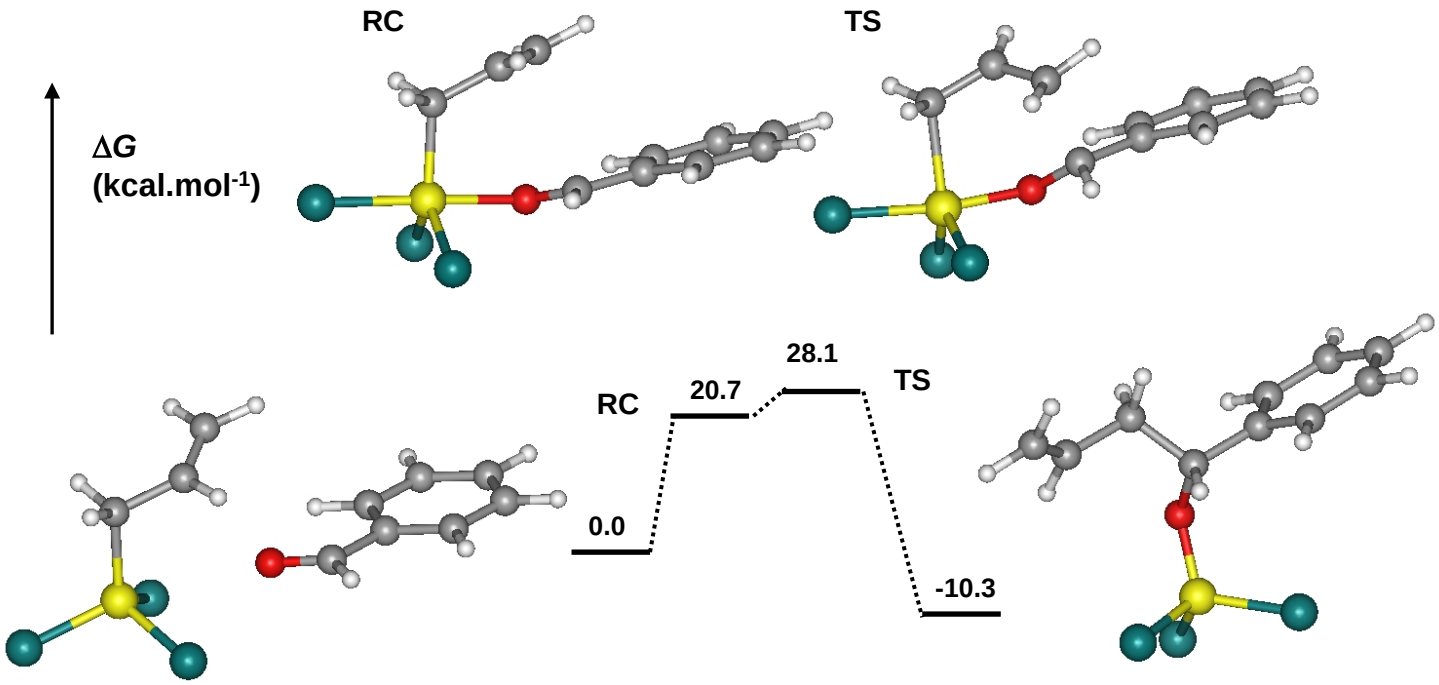

$\Delta E^{\ddagger}$ = 15.3 kcal.mol^{-1} …CCSD(T)/aug-cc-pVDZ
$\Delta E^{\ddagger}$ = 15.6 kcal.mol^{-1} …RI-DFT(PBE)+D/TZVPP

Pyridine-N-oxide: associative mechanism

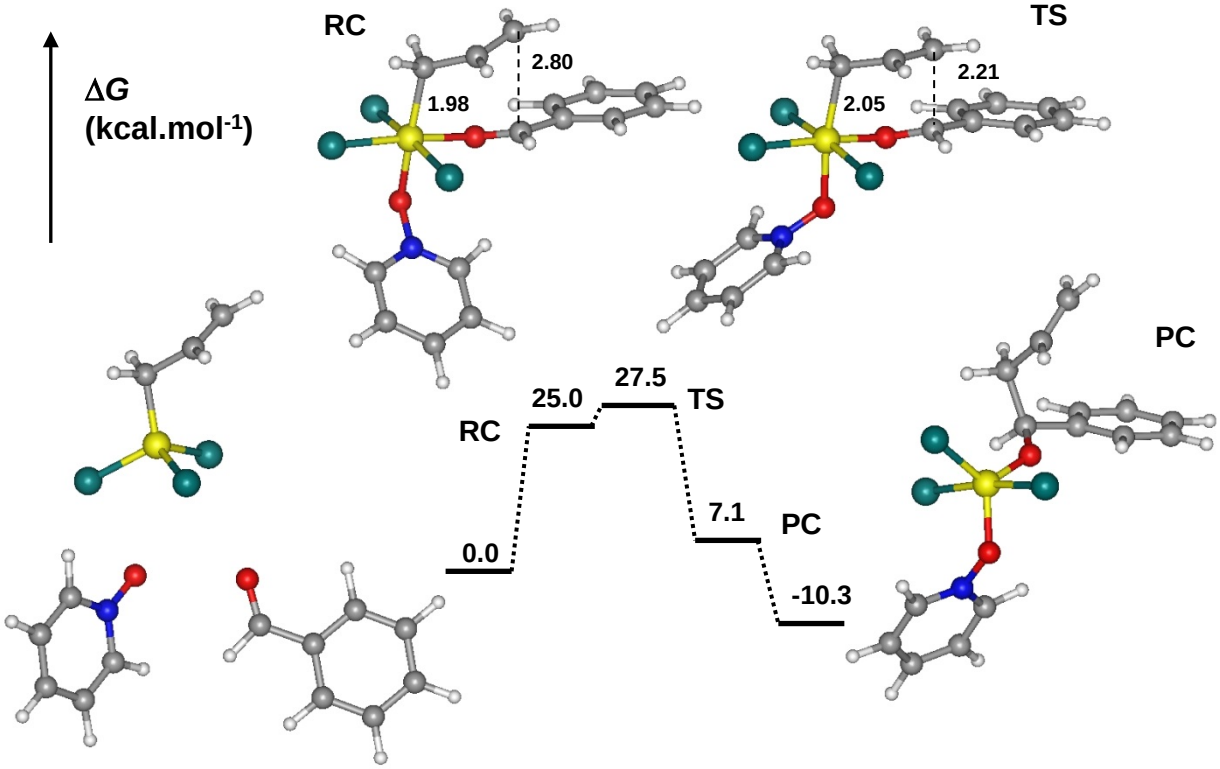

Second-sphere mechanism (ruled out)

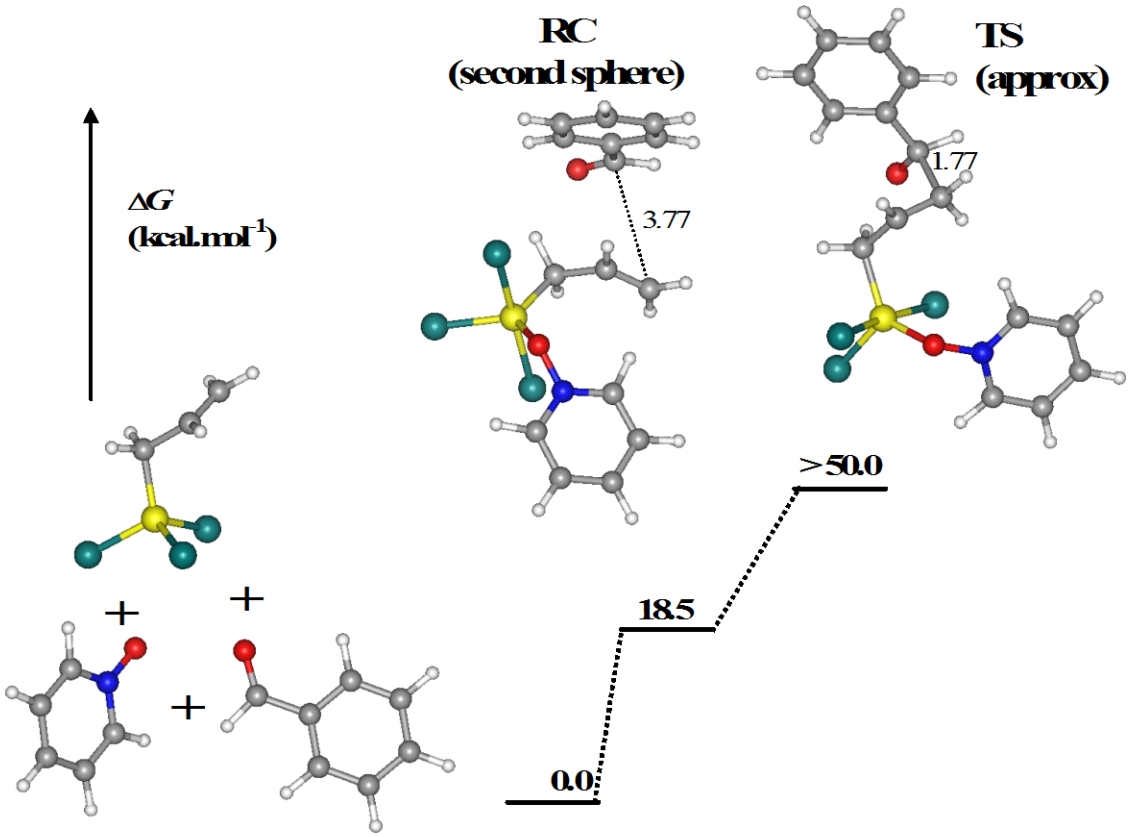

QUINOX Catalyst

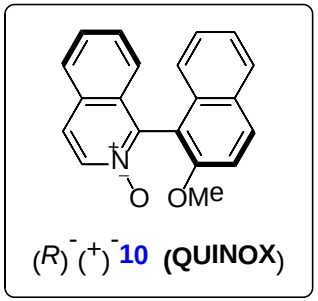

***ee (calc)* = 82%**

***ee (exp)* = 87%**

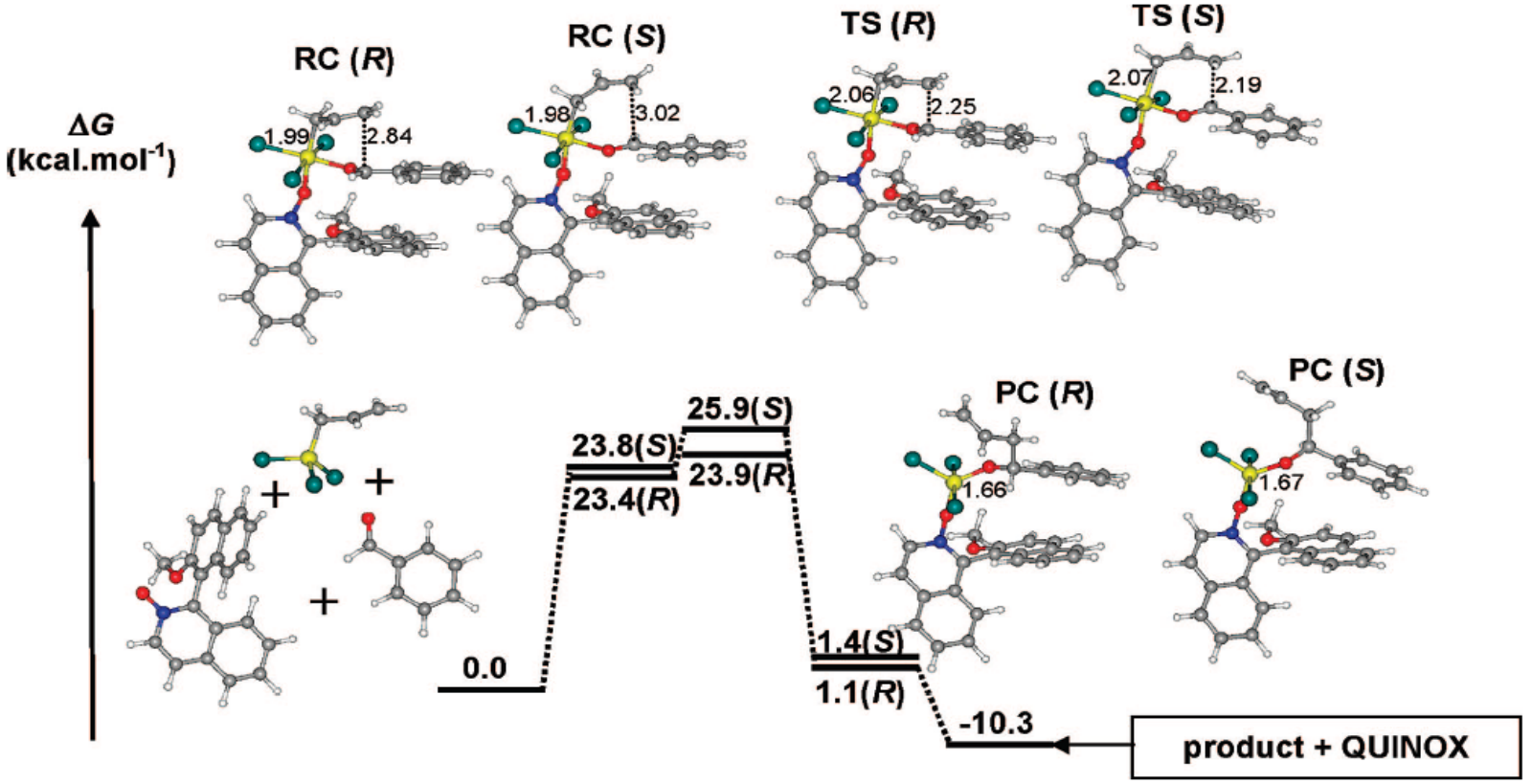

Figure 4. The equilibrium geometries of the most stable reactant complexes (RC), transition states (TS), and product complexes (PC) along the reaction coordinate for the associative pathway of allylation of benzaldehyde (**1a**) catalyzed by (*R*)-(+)-QUINOX (**9**). The calculated values for Δ*G* were obtained at the RI-PBE(+D)/TZVP//RI-PBE(+D)/6-31G(d) level; all distances are in Å.

Table: The calculated thermochemical data for METHOX as a catalyst. All values are in kcal.mol^{-1}.

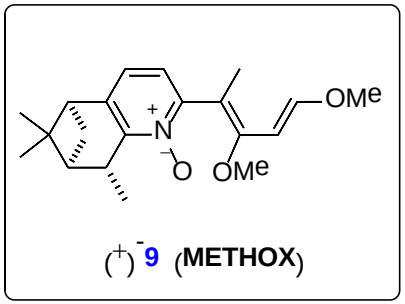

(±) **9** (**METHOX**)

mechanism	config.	reactant complex	transition state	product complex
associative	*R*	24.4	29.3	-2.0
	S	-[a]	28.7	-4.8
dissociative	*R*	25.0	25.6	-2.0
	S	17.8	23.3	-4.8

***ee (calc)* = 88%**

***ee (exp)* = 96%**

METHOX Catalyst

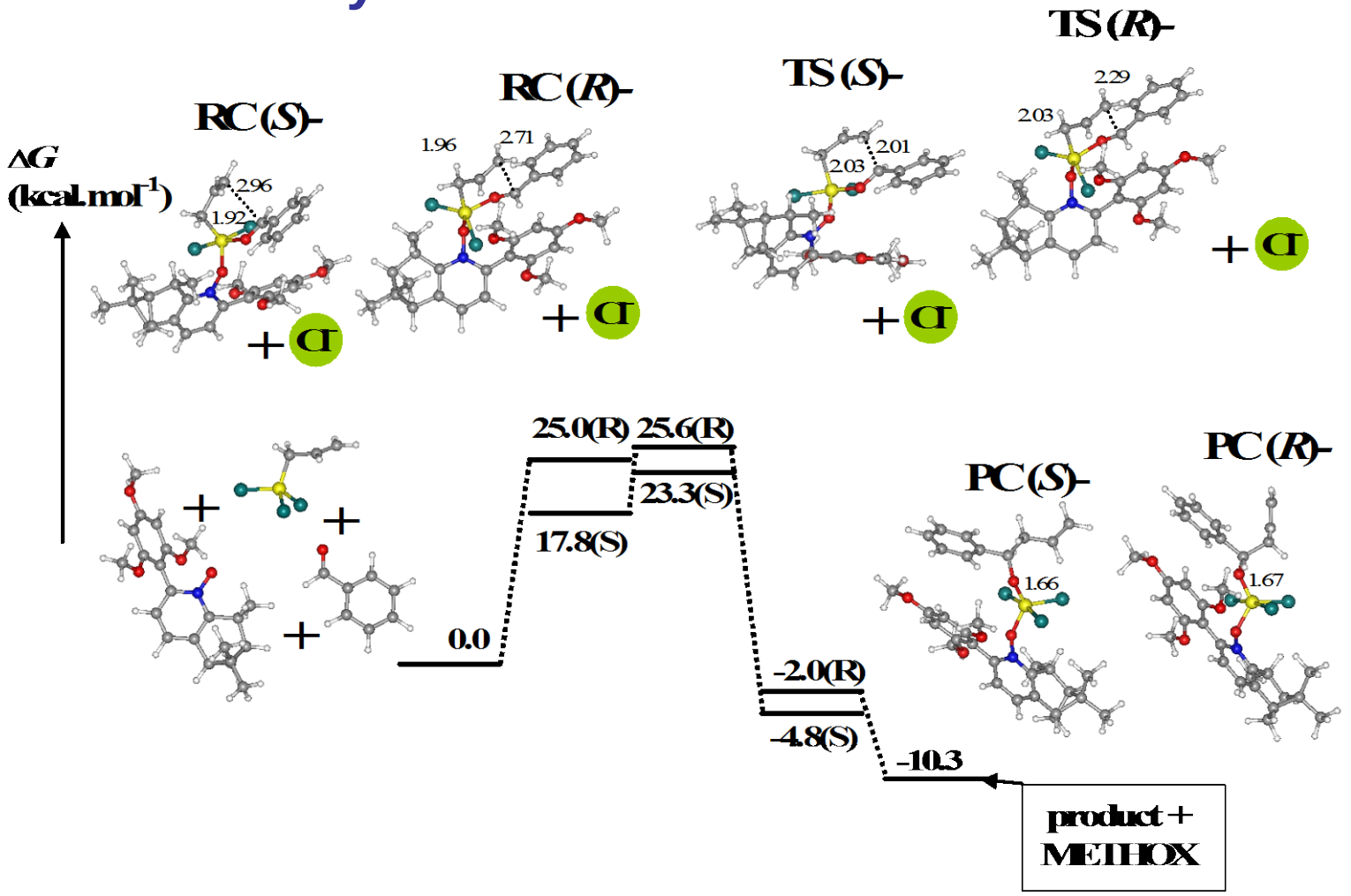

Malkov, A. V.; Stončius, S.; Bell, M.; Castelluzzo, F.; Ramírez-López, P.; Biedermannová, L.; Langer, V.; Rulíšek, L.; Kočovský, P.: *Chem. Eur. J.* **2013**, *19*, 9167-9185.

Origin of the stereoselectivity

Table: The decomposition of the free energy barriers into the contributions originating in zero-point energy corrections, entropy, solvation energies, and dispersion energies. All values are in kcal.mol^{-1}.

Catalyst	config	ΔE_{gp} [a]	ΔG_{solv} [b]	$\Delta(-T\Delta S)_{gp}$ [c]	ΔE_{disp} [d]
QUINOX	*R*	0.0	0.0	0.0	0.0
(associative TS)	*S*	-0.3	0.7	0.5	1.1
METHOX	*R*	0.0	0.0	0.0	0.0
(dissociative TS)	*S*	-3.2	-0.4	-0.6	1.9

[a] ΔE_{gp} is the difference in the *in vacuo* energies between R, S isomers
[b] ΔG_{solv} is the difference in solvation free energies between R, S isomers
[c] $\Delta(-T\Delta S)_{gp}$ is the difference in the *in vacuo* entropic terms between R, S isomers
[d] ΔE_{disp} is the difference in the dispersion energy stabilizations between R, S isomers

Mechanistic Dichotomy in the Asymmetric Allylation of Aldehydes with Allyltrichlorosilanes Catalyzed by Chiral Pyridine *N*-Oxides

Scheme 5. Mechanism of catalysls by chiral pyridine-*N*-oxides

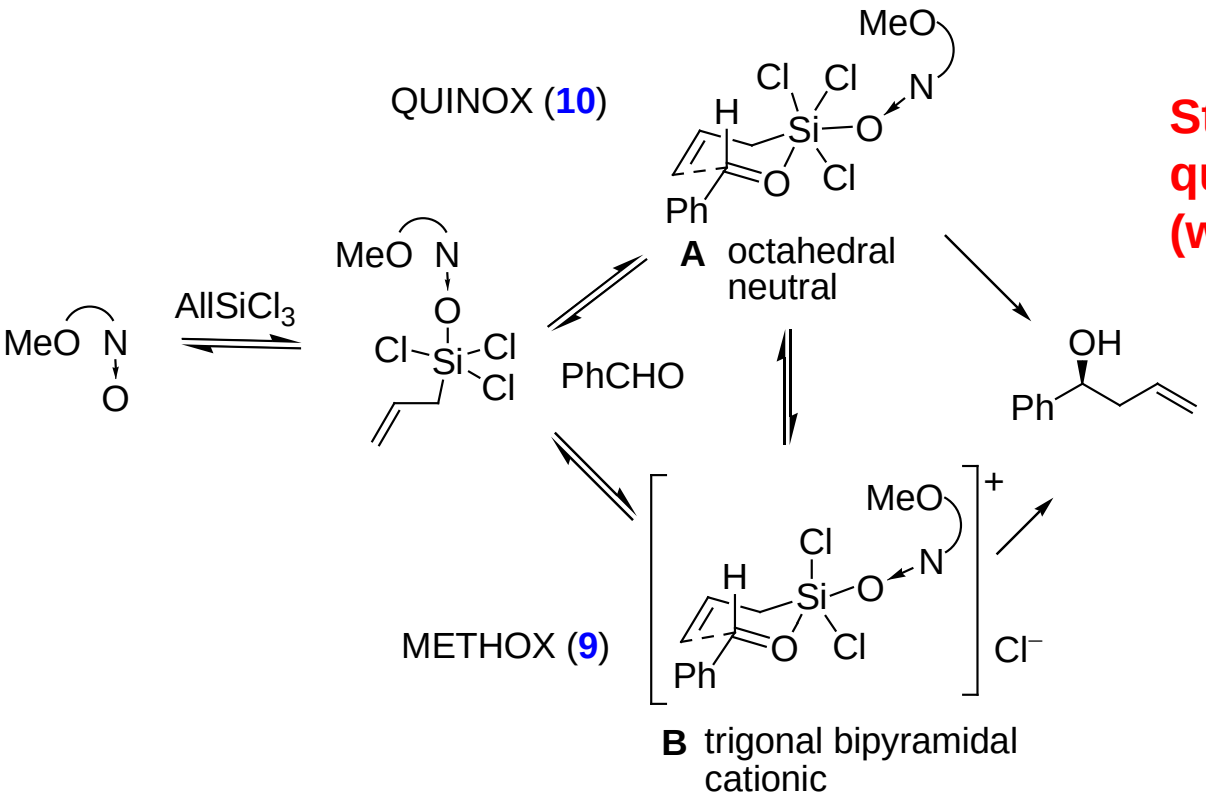

Stereoselectivities quantitatively predicted (within 1 kcal.mol^{-1})

Malkov, A. V.; Ramírez-López, P.; Biedermannová, L.; Rulíšek, L.; Dufková, L.; Kotora, M.; Zhu, F.; Kočovský, P.: *J. Am. Chem. Soc.* **2008**, *130*, 5341. Malkov, A. V.; Stončius, S.; Bell, M.; Castelluzzo, F.; Ramírez-López, P.; Biedermannová, L.; Langer, V.; Rulíšek, L.; Kočovský, P.: *Chem. Eur. J.* **2013**, *19*, 9167.

Summary and Outlook

Conformational complexity (competing reaction pathways)
Entropic effects (ideal gas + PCM solvation = ??, *Cl* $^{-}$ *translational entropy*)
Solvation Effects (non-innocent solvents, ionic systems, COSMO-RS)
Accuracy of TS barriers (2 kcal.mol^{-1} is optimistic error bar in medium-sized, well-defined models, while it can easily overcome 5 kcal.mol^{-1} in more complex systems)
…tunneling, “non-TST” systems,…

***En Route* from Quantitative Insight to Simpler Concepts?**

Qualitative Concepts (60’s – 80’s)

Towards Accurate Numbers (90’s -2012)

Quantitative Concepts (and Guidance for Experiments??)

Divergent Pathways and Competitive Mechanisms of Metathesis Reactions between 3-Arylprop-2-ynyl esters and Aldehydes

Trujillo, C.; Sánchez-Sanz, G.; Karpavičienė, I.; Jahn, U.; Čikotienė, I.; Rulíšek, L.: Divergent Pathways and Competitive Mechanisms of Metathesis Reactions between 3-Arylprop-2-ynyl esters and Aldehydes: An Experimental and Theoretical Study. *Chem. Eur. J.* **2014**, *20*, 10360-10370.

The formation of carbon–carbon bonds is at the heart of synthetic organic chemistry

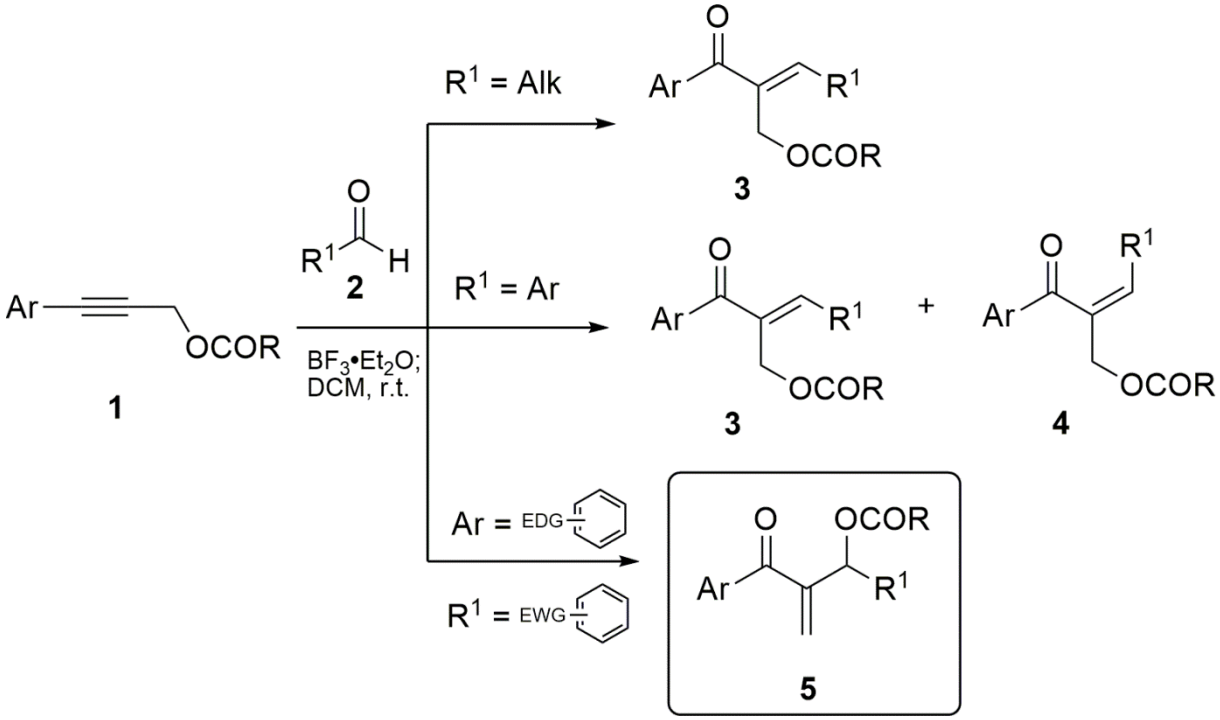

Experimental Data

Table 1. Reactions of selected 3-arylprop-2-ynyl esters (**1**) with ^{18}O-labeled aldehydes (**2**).

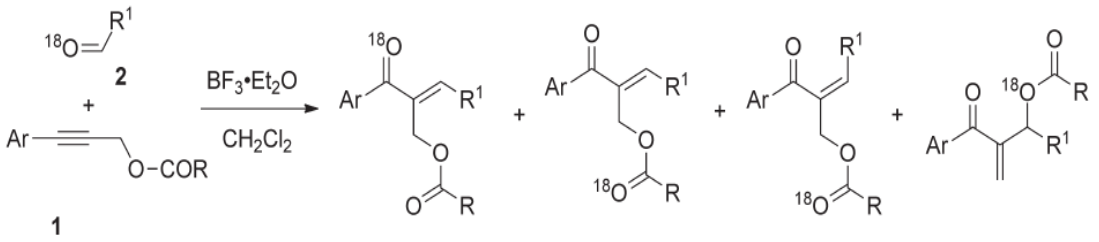

Entry	Alkyne			Aldehyde		Reaction time [h]	Products	Isolated overall yield [%]	3		4	5
	1	Ar	R	2	R^1				Labeled ketone	Labeled ester carbonyl		
1	**1a**	Ph	Me	**2a**	Me	24	**3aa**	27	1	1.8	–	–
2	**1a**	Ph	Me	**2b**	2-FC_6H_4	24	**3ab**, **4ab**	65	0.5	1.5	1	–
3	**1a**	Ph	Me	**2c**	2,4-$Cl_2C_6H_4$	24	**3ac**, **4ac**	71	–	2	1	–
4	**1b**	4-$MeOC_6H_4$	Me	**2d**	4-$NO_2C_6H_4$	5 min	**3bd**, **5bd**	89	–	0.15	–	1
5	**1c**	4-$MeOC_6H_4$	Ph	**2d**	4-$NO_2C_6H_4$	5 min	**5cd**[a]	78	–	–	–	1

[a] Hydrolyzed **5.1cd** with the ^{18}O-label in the hydroxy group was also isolated in 12% yield.

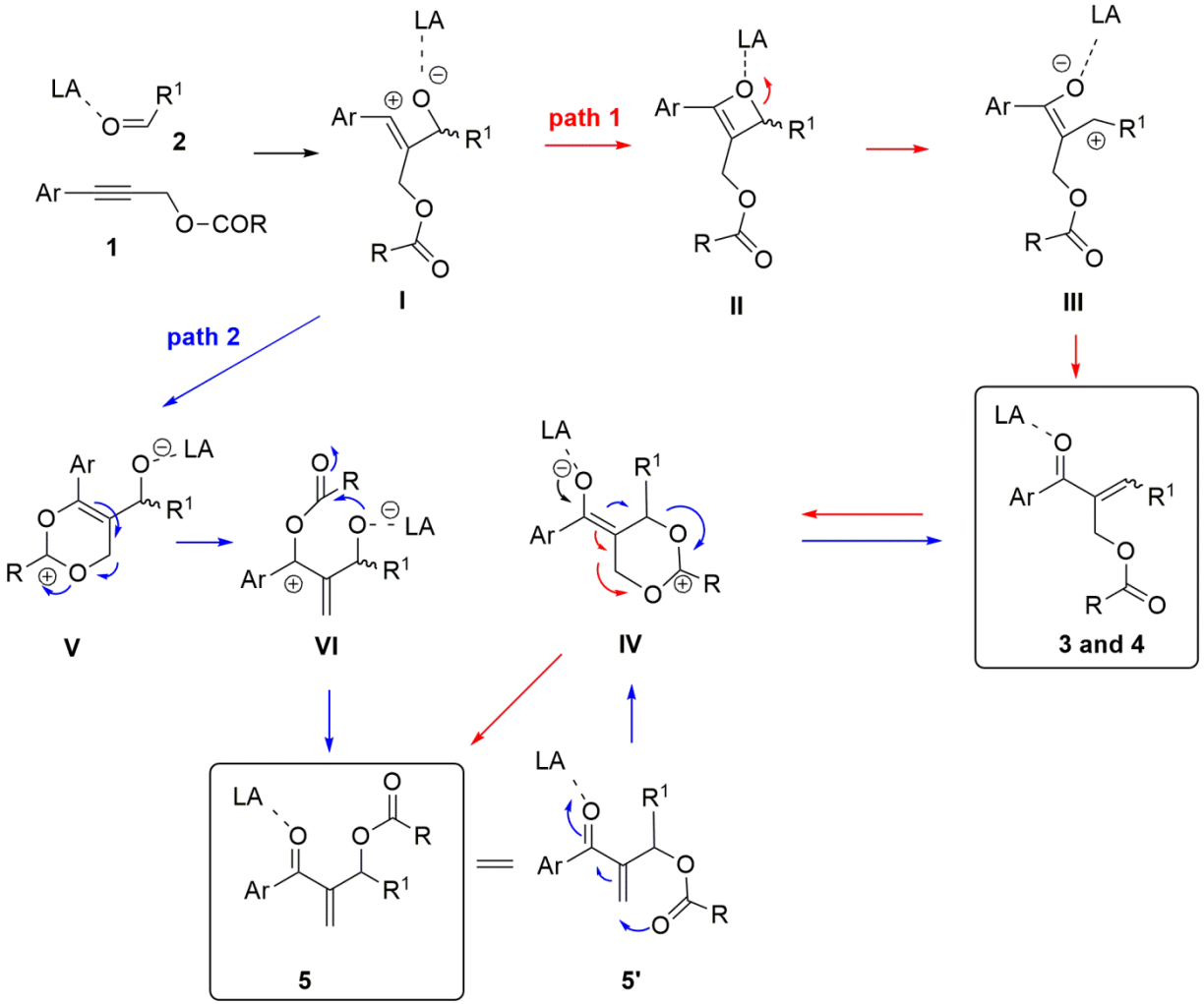

Scheme: Two plausible mechanistic pathways. Path 1 (**red arrows**): Classical alkyne–carbonyl metathesis route, followed by 1,3 carboxylate migration (as proposed originally). Path 2 (**blue arrows**): A novel nucleophilic addition/rearrangement cascade reaction. LA=$BF_3 \cdot Et_2O$. Depicted structures represent either energy minima or transition states.

Table 2. Reactions of selected 3-arylprop-2-ynyl esters **1** and aldehydes **2** with $BF_3{\cdot}OEt_2$ in CH_2Cl_2.

Entry	Alkyne	Aldehyde	Additive	T [°C]	Reaction time [h][a]	Product ratio	Overall yield [%]
1	**1a**	**2a**	–	20	24	**3aa**/**4aa**/**5aa** = 1:0:0	26[b]
2	**1a**	**2a**	TMSOTf[c]	−10	0.5	**3aa**/**4aa**/**5aa** = 1:0:0.3	16[b]
3	**1a**	**2b**	–	20	24	**3ab**/**4ab**/**5ab** = 2:1:0	77
4	**1a**	**2b**	TMSOTf[c]	−10	0.5	**3ab**/**4ab**/**5ab** = 5.3:1.1:1	69
5	**1a**	**2c**	–	20	24	**3ac**/**4ac**/**5ac** = 2:1:0	69
6	**1a**	**2c**	TMSOTf[c]	−10	0.5	**3ac**/**4ac**/**5ac** = 1:0:1.5	55
7	**1b**	**2d**	–	20	5 min	**3bd**/**4bd**/**5bd** = 0.15:0:1[d]	82
8	**1b**	**2d**	–	10	25 min	**3bd**/**4bd**/**5bd** = 1:0:1	51
9	**1b**	^{18}**O-2d**	–	20	24	**3bd**/**4bd**/**5bd** = 1.3:1:0	64

[a] Isolation of products was performed after full conversion of the starting alkyne **1**. [b] The low overall yields can be explained by possible self-condensation side reaction of the aliphatic aldehyde under the reaction conditions. [c] To solve the problem of slow reactivity of the starting materials at lower temperatures we used the synergistic couple of $BF_3{\cdot}Et_2O$ and TMSOTf. [d] Compounds **3bd** and **5bd** were isolated as a mixture due to their similiar R_f values. The product ratio was determined from the ^{1}H NMR spectrum.

Computations: Benchmarking Against CCSD(T) => ωB97XD functional + COSMO-RS

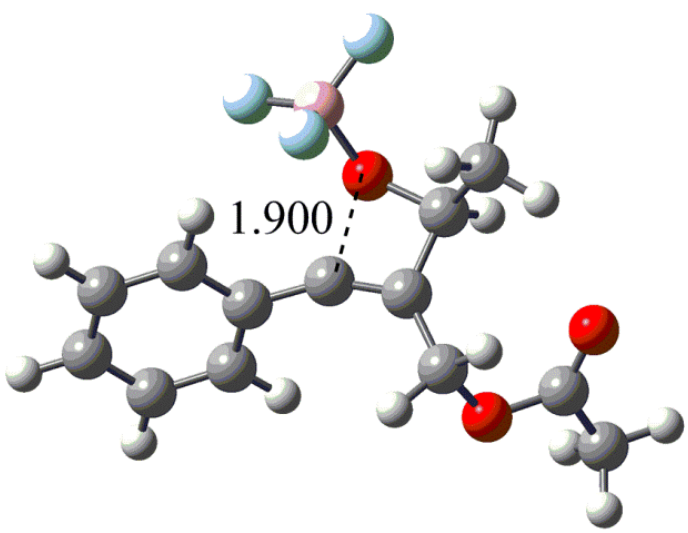

TS I_II

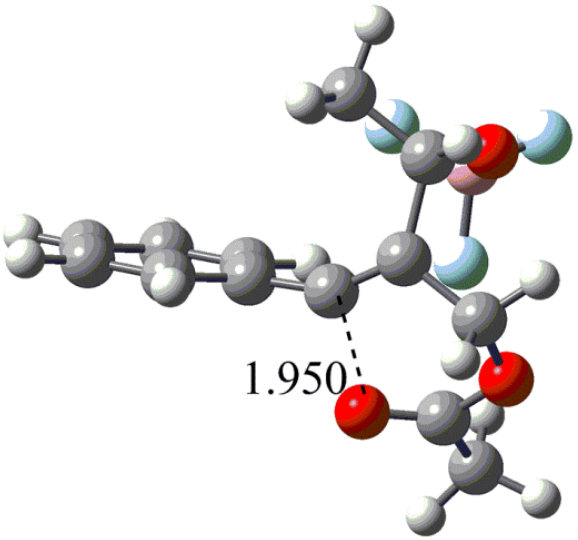

TS I_V

Figure: The equilibrium geometries of two key transition states that divert the reaction to path 1 or 2.

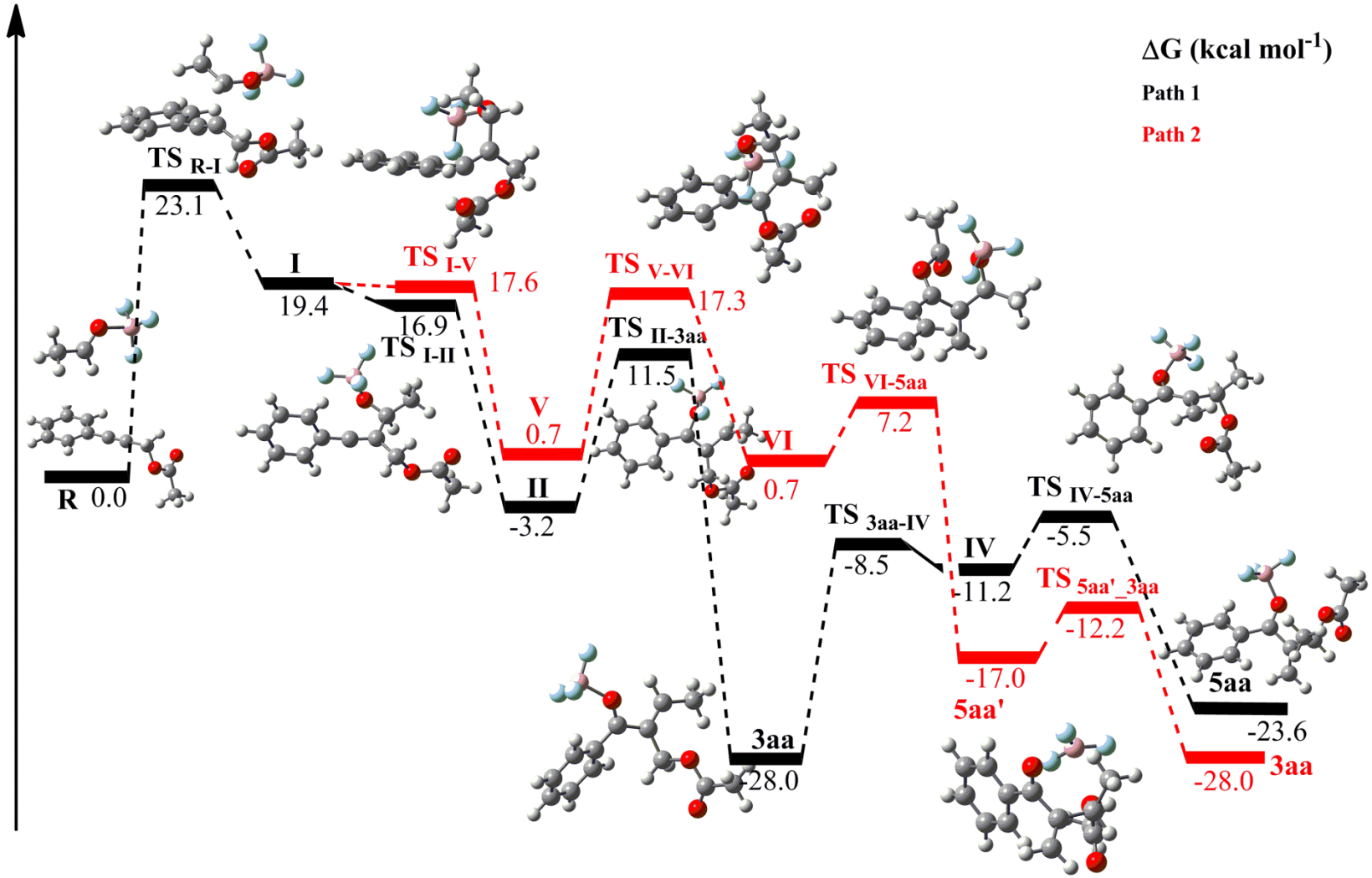

Figure. Gibbs energy levels for paths 1 (black) and 2 (red) calculated at the DFT(wB97XD)/6-311 G(2d,p)//RI-PBED3/def2-SVP level of theory and COSMO-RS solvation method for the reaction between **1a** and **2a**.

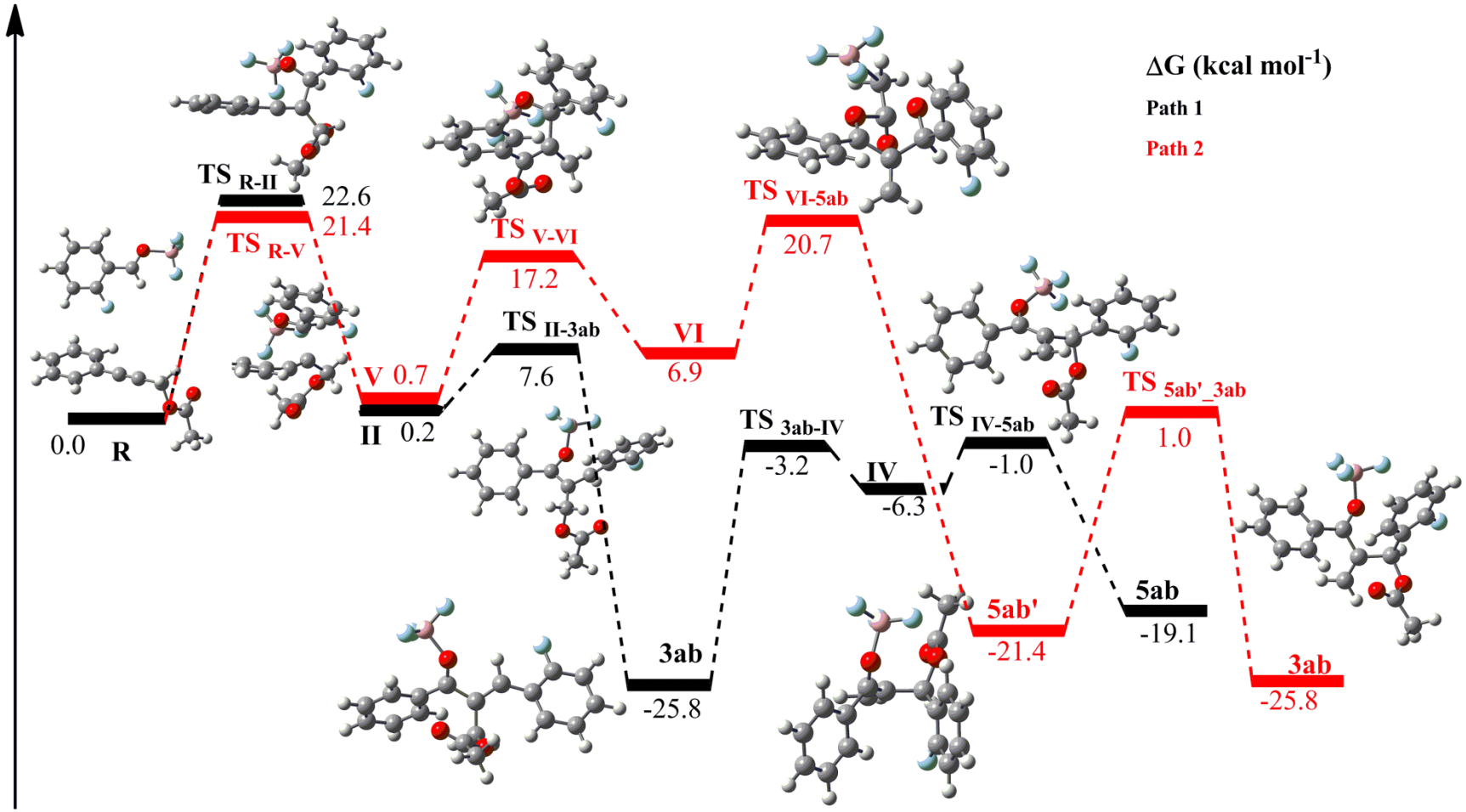

Figure. Gibbs energy levels for paths 1 (black) and 2 (red) calculated at the DFT(wB97XD)/6-311 G(2d,p)//RI-PBED3/def2-SVP level of theory and COSMO-RS solvation method for the reaction between **1a** and **2b**.

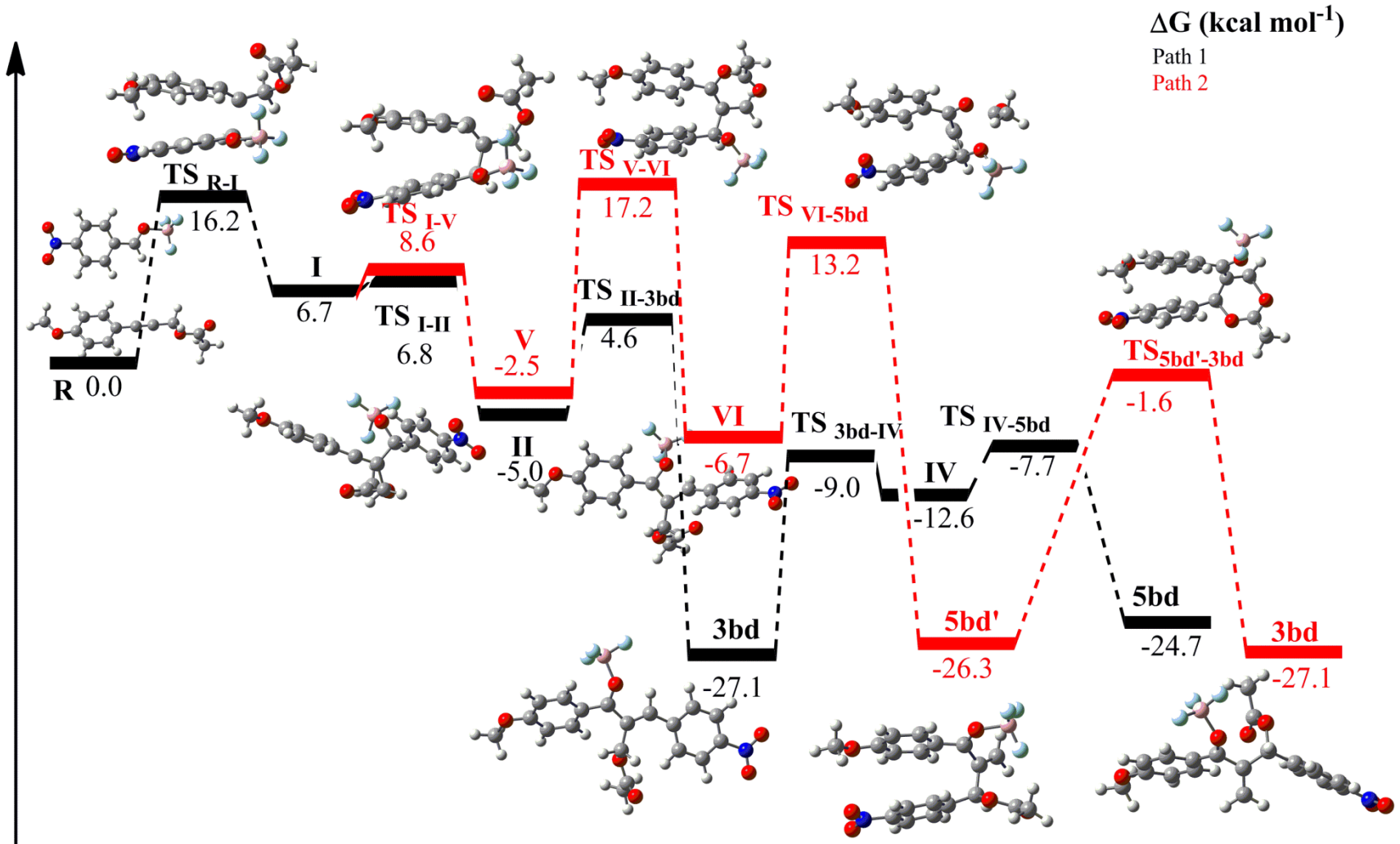

Figure. Gibbs energy levels for paths 1 (black) and 2 (red) calculated at the DFT(wB97XD)/6-311 G(2d,p)//RI-PBED3/def2-SVP level of theory and COSMO-RS solvation method for the reaction between **1b** and **2d**.

Explicit Models for Condensed Phases

Partition function

$$Q = \int\int e^{-E(\mathbf{q},\mathbf{p})/k_\mathrm{B}T}\, d\mathbf{q}d\mathbf{p}$$

Statistical Thermodynamics (Lecture 5)

$$U = k_\mathrm{B}T^2 \left(\frac{\partial \ln Q}{\partial T}\right)_V$$

$$P = k_\mathrm{B}T \left(\frac{\partial \ln Q}{\partial V}\right)_T$$

$$H = U + PV$$

$$A = -k_\mathrm{B}T \ln Q$$

$$S = k_\mathrm{B}T \left(\frac{\partial \ln Q}{\partial T}\right)_V + k_\mathrm{B} \ln Q$$

$$G = H - TS$$

We may rewrite *U* as

$$U = \frac{\int\int E(\mathbf{q},\mathbf{p}) e^{-E(\mathbf{q},\mathbf{p})/k_\mathrm{B}T} d\mathbf{q}d\mathbf{p}}{\int\int e^{-E(\mathbf{q},\mathbf{p})/k_\mathrm{B}T} d\mathbf{q}d\mathbf{p}}$$

$$= \int\int E(\mathbf{q},\mathbf{p}) P(\mathbf{q},\mathbf{p}) d\mathbf{q}d\mathbf{p}$$

Carrying Monte Carlo or MD

$$\langle U\rangle_\mathrm{B} - \langle U\rangle_\mathrm{A} = \frac{1}{M_\mathrm{B}} \sum_i^{M_\mathrm{B}} E_i - \frac{1}{M_\mathrm{A}} \sum_i^{M_\mathrm{A}} E_i$$

$$= \langle E\rangle_\mathrm{B} - \langle E\rangle_\mathrm{A}$$

Analogously, for *A*

$$A = k_{\mathrm{B}}T \ln \frac{1}{Q}$$

$$= k_{\mathrm{B}}T \ln \left[\frac{\int\int e^{E(\mathbf{q},\mathbf{p})/k_{\mathrm{B}}T} e^{-E(\mathbf{q},\mathbf{p})/k_{\mathrm{B}}T} d\mathbf{q}d\mathbf{p}}{\int\int e^{-E(\mathbf{q},\mathbf{p})/k_{\mathrm{B}}T} d\mathbf{q}d\mathbf{p}} \right]$$

$$= k_{\mathrm{B}}T \ln \left[\int\int e^{E(\mathbf{q},\mathbf{p})/k_{\mathrm{B}}T} P(\mathbf{q},\mathbf{p}) d\mathbf{q}d\mathbf{p} \right]$$

Carrying Monte Carlo or MD

$$\langle A \rangle_{\mathrm{B}} - \langle A \rangle_{\mathrm{A}} = k_{\mathrm{B}}T \ln \left(\frac{1}{M_{\mathrm{B}}} \sum_{i}^{M_{\mathrm{B}}} e^{E_i/k_{\mathrm{B}}T} \right) - k_{\mathrm{B}}T \ln \left(\frac{1}{M_{\mathrm{A}}} \sum_{i}^{M_{\mathrm{A}}} e^{E_i/k_{\mathrm{B}}T} \right)$$

$$= k_{\mathrm{B}}T \ln \left\langle e^{E/k_{\mathrm{B}}T} \right\rangle_{\mathrm{B}} - k_{\mathrm{B}}T \ln \left\langle e^{E/k_{\mathrm{B}}T} \right\rangle_{\mathrm{A}}$$

$$= k_{\mathrm{B}}T \ln \left(\frac{\left\langle e^{E/k_{\mathrm{B}}T} \right\rangle_{\mathrm{B}}}{\left\langle e^{E/k_{\mathrm{B}}T} \right\rangle_{\mathrm{A}}} \right)$$

Free Energy Perturbation (Zwanzig, 1954)

$$\langle A \rangle_B - \langle A \rangle_A = k_B T \ln \left\langle e^{(E_B - E_A)/k_B T} \right\rangle_A$$

Example: HCN → HNC reaction

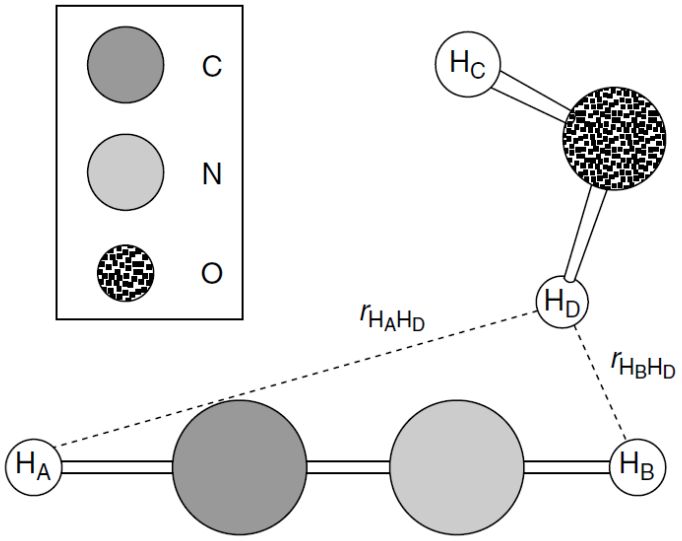

In practice, a simulation windows for each coupling parameter

$$E(\lambda) = \lambda E_{\mathrm{B}} + (1-\lambda) E_{\mathrm{A}}$$

$$\langle A \rangle_{\mathrm{B}} - \langle A \rangle_{\mathrm{A}} = \sum_{\lambda=0}^{1} k_{\mathrm{B}} T \ln \left\langle e^{(E_{\lambda+d\lambda} - E_{\lambda})/k_{\mathrm{B}}T} \right\rangle_{\lambda}$$

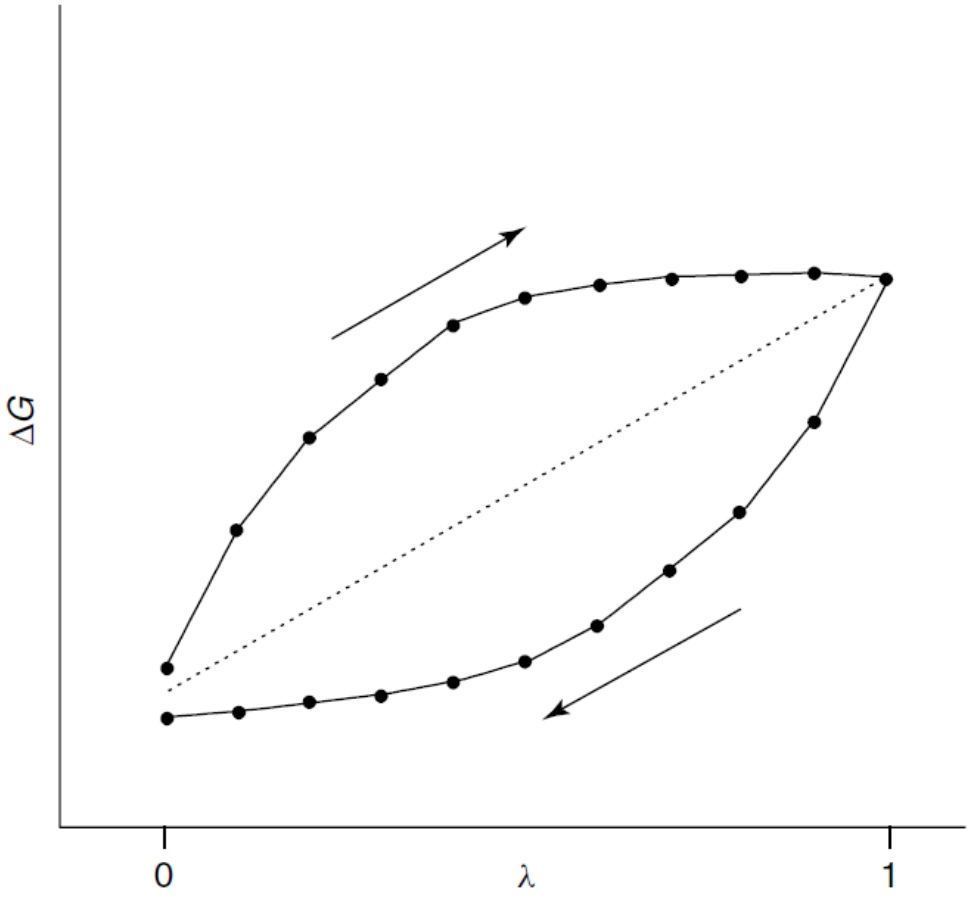

Figure 12.2 A typical FEP diagram showing the free-energy change in the forward (above) and reverse (below) directions for a λ-coupled mutation

Slow Growth Method

$$\langle A\rangle_{\mathrm{B}} - \langle A\rangle_{\mathrm{A}} = \lim_{d\lambda\to 0} \sum_{\lambda=0}^{1} k_{\mathrm{B}}T \ln\left\langle 1 + \frac{(E_{\lambda+d\lambda} - E_{\lambda})}{k_{\mathrm{B}}T}\right\rangle_{\lambda}$$

$$\langle A\rangle_{\mathrm{B}} - \langle A\rangle_{\mathrm{A}} = \lim_{d\lambda\to 0} \sum_{\lambda=0}^{1} k_{\mathrm{B}}T \left\langle \frac{(E_{\lambda+d\lambda} - E_{\lambda})}{k_{\mathrm{B}}T}\right\rangle_{\lambda}$$

$$= \lim_{d\lambda\to 0} \sum_{\lambda=0}^{1} \langle (E_{\lambda+d\lambda} - E_{\lambda})\rangle_{\lambda}$$

$$= \lim_{d\lambda\to 0} \sum_{\lambda=0}^{1} (E_{\lambda+d\lambda} - E_{\lambda})$$

Thermodynamic Integration

$$\langle A\rangle_{\mathrm{B}} - \langle A\rangle_{\mathrm{A}} = \lim_{d\lambda\to 0}\sum_{\lambda=0}^{1}\langle (E_{\lambda+d\lambda} - E_{\lambda})\rangle_{\lambda}$$

$$= \lim_{\Delta\lambda\to 0}\sum_{\lambda=0}^{1}\left\langle \frac{(E_{\lambda+\Delta\lambda} - E_{\lambda})}{\Delta\lambda}\right\rangle_{\lambda}\Delta\lambda$$

$$= \int_{0}^{1}\left\langle \frac{\partial E}{\partial\lambda}\right\rangle_{\lambda} d\lambda$$

$$\approx \sum_{\lambda=0}^{1}\left\langle \frac{\partial E}{\partial\lambda}\right\rangle_{\lambda}\Delta\lambda$$

Potential of Mean Force